# *Clostridium perfringens* type A enterotoxin forms mepacrine-sensitive pores in pure phospholipid bilayers in the absence of putative receptor proteins

Simon P. Hardy [a],*, Christie Ritchie [a], Marcus C. Allen [a], Richard H. Ashley [b], Per Einar Granum [c]

[a] *Department of Pharmacy and Biomolecular Sciences, University of Brighton, Lewes Road, Brighton, Sussex BN2 4GJ, UK*
[b] *Department of Biomedical Sciences, University of Edinburgh, Edinburgh, UK*
[c] *Department of Pharmacology, Microbiology and Food Hygiene, Norwegian School of Veterinary Science, P.O. Box 8146, Oslo, Norway*

## Abstract

*Clostridium perfringens* enterotoxin (CPE) is an important cause of food poisoning with no significant homology to other enterotoxins and its mechanism of action remains uncertain. Although CPE has recently been shown to complex with tight junction proteins, we have previously demonstrated that CPE increases ionic permeability in single Caco-2 cells using the whole-cell patch-clamp technique, thereby excluding any paracellular permeability. In this paper we demonstrate that CPE forms pores in synthetic phospholipid membranes in the absence of receptor proteins. The properties of the pores are consistent with CPE-induced permeability changes in Caco-2 cells suggesting that CPE has innate pore-forming ability. © 2001 Elsevier Science B.V. All rights reserved.

*Keywords:* Food poisoning; Pore-forming toxin; Planar lipid bilayer

## 1. Introduction

Food poisoning caused by *Clostridium perfringens* type A is due to the action of a 35 kDa enterotoxin, CPE, which is produced when the organism sporulates in the intestine. The enterotoxic activity of CPE has been demonstrated by its ability to induce diarrhoea and abdominal cramps in human volunteers, and marked fluid accumulation in isolated animal intestinal loops [1,2]. In vitro studies have shown that CPE increases membrane ion permeability in a number of cell lines, including Caco-2, Vero (monkey kidney epithelium) cells and rabbit hepatocytes [3], but its mechanism of action remains unclear. It is suggested that CPE acts in a manner distinct from other enterotoxins, in that it interacts with host cell membrane proteins to form 'small' and 'large complexes' [4]. Putative receptors have been identified (claudin-4 [5] and claudin-3 [6]), both integral components of tight junctions. Whether claudins represent true receptors is uncertain [7]. Occludin can also complex with CPE but this does not confer susceptibility to CPE in transfected cells [8]. It is possible that junction proteins only become bound to CPE as a secondary event.

Sonada et al. [9] reported a fall in transepithelial resistance (TER) in MDCK cells after application of a COOH fragment peptide of CPE but only when added to the basolateral side. Apical exposure did not reduce TER. We recently described increases in short-circuit current along with marked falls in TER in intestinal Caco-2 monolayers in Ussing chambers following exposure of the apical membrane to purified, intact CPE [10]. In addition we demonstrated increases in ionic permeability in single cells using whole-cell patch clamp [10]. In contrast to short-circuit measurements, whole-cell currents are not contaminated by paracellular permeability. In the present study we set out to determine whether CPE can form transmembrane pores in pure planar lipid bilayers, and if their properties correlated with our findings in Caco-2 cells. We showed that CPE can induce ion channels in pure lipid bilayers devoid of any putative receptor proteins, and these channels have similar properties to those observed in Caco-2 cells.

## 2. Methods

### 2.1. C. perfringens enterotoxin

*C. perfringens* type A enterotoxin was purified as described [11] and redissolved from a 15% (w/v) ammonium sulphate precipitate in 20 mM phosphate buffered saline (PBS, pH 7.2), and dialysed overnight at 4°C against PBS. Toxin concentration was estimated by UV absorbance (Ex = 1.33 mg$^{-1}$·cm$^2$ [11]). The working stock solution of CPE was stored at 4°C at a concentration of $\sim 0.5$ mg/ml, to minimise aggregation.

### 2.2. Planar lipid bilayer recording

Planar lipid bilayer recordings were carried out using a system described previously [12]. Pure synthetic lipids (Avanti Polar Lipids, Birmingham, AL, USA) were dispersed in chloroform and stored at −70°C under nitrogen. Briefly, lipid bilayers were formed from a dispersion of 15 mg/ml palmitoyloleoylphosphatidylethanolamine and 15 mg/ml palmitoyloleoylphosphatidylserine in *n*-decane, which

was drawn across a 0.4 mm diameter hole in a polystyrene cup separating two solution-filled chambers, designated *cis* and *trans*. The *cis* chamber (to which the toxin and drugs were added) was held at ground (0 mV), and the *trans* chamber was clamped to a range of potentials using a GeneClamp 500 patch-clamp amplifier equipped with a CV-5B (100 GΩ) bilayer headstage (Axon Instruments). The sign of the membrane potential refers to the *trans* chamber, and currents are defined as 'positive' when cations flow from *trans* to *cis*. Transmembrane currents were low-pass filtered at 500 Hz (8 pole Bessel) digitised at 5 kHz, and recorded directly to computer disk via a Digidata 1200 AD interface (Axon Instruments). Membrane capacitance was measured by differentiating a triangle wave input of 0.2 kHz. Only bilayers that had a conductance of less than 10 pS and initial capacitance of at least 300 pF were used. Unless otherwise stated, lipid bilayers were bathed in 100 mM NaCl containing 5 mM HEPES/NaOH (pH 7.3), and all recordings were made at room temperature (19–22°C).

### 2.3. Channel analysis

30–180 s recordings were carried out for each holding potential and analysed off-line using PAT v7.0 software (Strathclyde Electrophysiology Software). Maximum current amplitudes were determined from the peaks of Gaussian functions fitted to amplitude histograms, and for single-channel recordings integration of these histograms yielded the probability of a channel being open ($P_o$). Event transitions were detected by setting a threshold at 50% of the maximum current amplitude, and channel lifetimes were calculated from exponential fits to dwell time histograms. Ionic permeabilities relative to Na$^+$ ($P_x/P_{Na}$) were calculated using the reduced Goldman equation:

$$E_{rev} = \frac{RT}{F} \ln \frac{\left([Na^+]_c + \left(\frac{P_x}{P_{Na}}\right) \cdot [X]_c\right)}{\left([Na^+]_t + \left(\frac{P_x}{P_{Na}}\right) \cdot [X]_t\right)}$$

where $E_{rev}$ is the measured reversal potential (mV), *t* is *trans*, *c* is *cis* (ground) and X is the replacement cation. *R*, *T* and *F* have their usual significance.
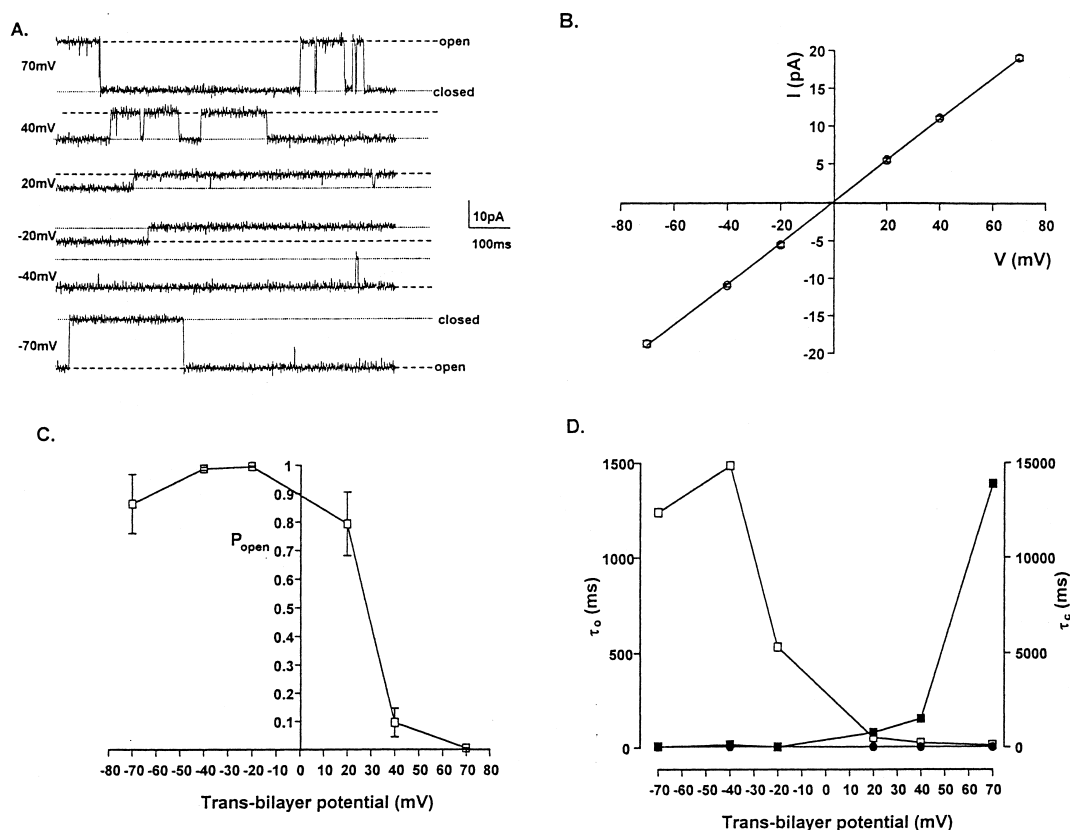
Fig. 1. Single-channel currents. (A) Recordings from a planar lipid bilayer after adding 10 μg CPE to the *cis* (ground) chamber. Bathing solution was symmetrical 100 mM NaCl, 5 mM HEPES/NaOH (pH 7.2). Applied voltages are given, and the open and closed levels are indicated by the dashed and dotted lines respectively. Note the reversal in the direction of current between negative and positive voltages. (B) Current–voltage (*I–V*) relationship of CPE-induced channels bathed in 100 mM NaCl. Values represent mean ± S.E.M. of nine bilayers. The solid line is plotted by regression analysis, and from the slope, the single-channel conductance is 270 ± 2 pS (mean ± S.E.M.). Note that the error bars are hidden within the symbols. (C) Voltage-dependent closure of CPE-induced channels. Single-channel open probability ($P_o$) plotted versus applied voltage demonstrates the tendency of the channels to close at voltages over +10 mV. (D) Channel lifetime analysis. Mean open and closed lifetimes of typical CPE-induced single-channel recordings, plotted versus applied voltage. As the applied voltage becomes more positive, the mean open time ($\tau_o$; □) decreases, and the mean duration of the longer closed times ($\tau_c$; ■) increases. The duration of the brief closed times (mean lifetime < 10 ms, ●) does not change.

## 3. Results

### 3.1. CPE-induced unit currents

Addition of up to 10 μg CPE to the *cis* bilayer chamber resulted in the appearance of rectangular current fluctuations, as shown in Fig. 1A. At similar concentrations of CPE channels inserted in ∼50% of all bilayers used. The time taken for single-channel current steps to appear was generally between 20 and 40 min, but ranged from 5 to 60 min. When more than one channel incorporated, the step increases in current were of uniform magnitude at equivalent positive and negative holding potentials (as shown in Fig. 1A).

Single-channel amplitudes were determined from the peaks of amplitude histograms fitted to Gaussian functions, and a combined current–voltage (*I–V*) relationship from nine independent experiments is shown in Fig. 1B. The data are fitted to a straight line giving a single-channel slope conductance of 270 ± 2 pS in 100 mM NaCl (mean ± S.E.M., *n* = 9).

### 3.2. Channel orientation and lifetimes

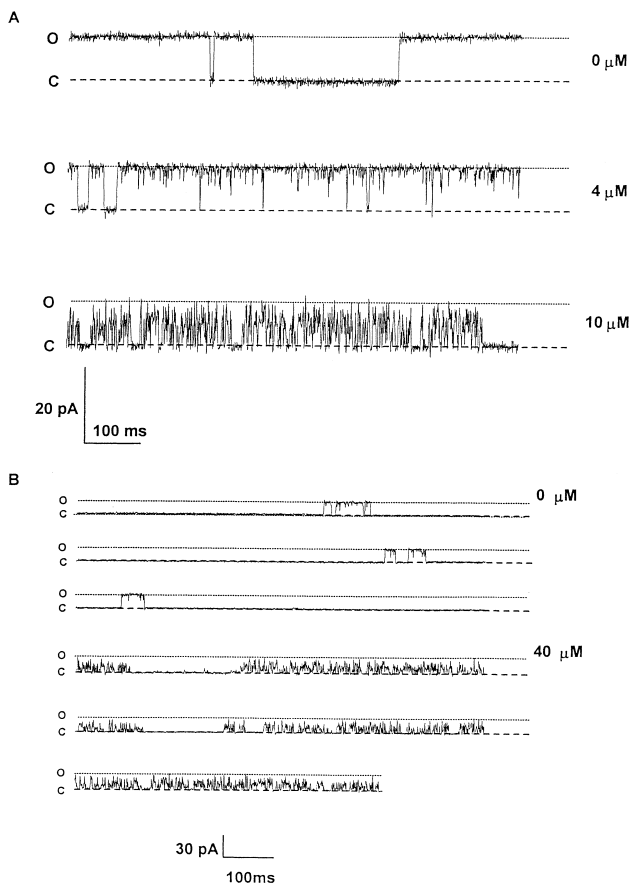Channel activity was noted to be voltage depen-

Fig. 2. Mepacrine block. (A) Representative sequential recordings from a single bilayer to show the development of 'flicker'-type block following the addition of increasing concentrations of mepacrine. Note that with 10 μM mepacrine the current amplitude does not reach the full open level. Bilayer held at +70 mV. Open and closed levels are indicated. (B) The top three traces show a contiguous recording trace from a single channel in 100 mM NaCl at +70 mV. Note the occasional appearance of channel openings. The lower three traces show a contiguous recording 60 s after adding 40 μM mepacrine to the *cis* (ground) chamber. Note the pronounced 'flicker' (as individual blocker molecules bind and unbind) and apparent reduced amplitude because openings between individual blocking events are too brief to be fully resolved.

dent (Fig. 1C). The channels were mainly open at negative membrane potentials ($P_o = 0.87$ at $-70$ mV) but tended to close at potentials greater than $+30$ mV ($P_o < 0.1$ at $+70$ mV). This voltage-sensitive behaviour provided a strong clue to the orientation of individual channels in the bilayer, and indicated that most channels incorporated in a preferred orientation. Very occasionally (in approx. 5% of the bilayers in which channels became incorporated),

unit currents showed the reverse pattern of voltage sensitivity (i.e. the channels tended to close at $-70$ mV rather than at $+70$ mV).

Mean open and closed single-channel lifetimes were determined by fitting exponential distributions to histograms of open and closed dwell times. At negative potentials, when the channel was mostly open, the mean open time ($\tau_o$) was 1239 ms at $-70$ mV. At positive potentials ($+70$ mV), the channel tended to close after briefer openings, with a reduced $\tau_o$ of only 15 ms (e.g. Fig. 1D). Closed time analysis was consistent with at least two components, including a short closed time of $< 10$ ms, illustrated by typical 'bursting' behaviour in which channel openings were separated by long periods of closure in single channel recordings (e.g. Fig. 2B).

### 3.3. The ionic selectivity of CPE channels

We investigated the selectivity of the pore for different monovalent ions. Complete replacement of 100 mM $Cl^-$ with the larger ion gluconate$^-$ reduced the single-channel conductance only marginally ($250 \pm 4$ pS, mean $\pm$ S.E.M.; $n = 4$ bilayers). Complete replacement of 100 mM $Na^+$ with $K^+$ more than doubled the single-channel conductance to $565 \pm 15$ pS (mean $\pm$ S.E.M., $n = 3$) whereas detectable channel activity was temporarily abolished by complete replacement with $N$-methyl-D-glucamine$^+$ (7.3 Å), channel activity returning upon replacement with NaCl (data not shown). Intermediate sized cations were examined by replacing 80 mM $Na^+$ on one side of the bilayer with organic cations of geometric mean diameters: dimethylamine$^+$ (4.4 Å), diethanolamine$^+$ (6.0 Å) and choline$^+$ (6.6 Å). Relative

Table 1
Ion selectivity of CPE-induced pores in lipid bilayers

| Ion ($n$) | Size (Å) | $E_{rev}$ (mV) | $P_x/P_{Na}$ |
|---|---|---|---|
| Dimethylammonium$^+$ (3) | 4.4 | $+10 \pm 2$ | 0.59 |
| Diethylammonium$^+$ (3) | 6.0 | $+12 \pm 2$ | 0.52 |
| Choline$^+$ (4) | 6.6 | $+25 \pm 4$ | 0.21 |

The selectivity of the CPE-induced pores to different cations with the number of bilayer experiments for each cation are given in parentheses ($n$) and the geometric mean diameter of the cation (Å). The reversal potentials ($\pm$S.E.M.) and calculated permeability ratios were obtained in asymmetric concentrations of $Na^+$ (mM) 100:20 *cis*:*trans*, with 80 mM of the replacement ion in the *trans* chamber.

permeability ratios ($P_x$:$P_{Na}$) were calculated from reversal potentials using the modified Goldman equation (see Section 2). In each case, the reversal potential was obtained by extrapolation from $I$–$V$ plots. Table 1 shows a clear fall in permeability ratios as the mean diameter of the replacement cation increases. This sequence mirrors that obtained in Caco-2 monolayers exposed to CPE [10].

### 3.4. Channel block by mepacrine

The pores formed by the ADP-ribosylating C2 toxin of *Clostridium botulinum* in planar bilayers [13] are inhibited by $\sim 20$ μM chloroquine, and we examined the ability of the structurally similar compound mepacrine (quinacrine) to inhibit CPE-induced single-channel currents. Addition of 4 μM mepacrine to the *cis* chamber resulted in a 'flicker-type' block of the channel, as illustrated in Fig. 2, and the effect was very marked with 40 μM mepacrine, which eventually resulted in permanent closure of the channels. Channel block appeared to be independent of membrane voltage (at least between holding potentials of $\pm 80$ mV).

## 4. Discussion

Using pure, synthetic phospholipids completely devoid of protein components, we have shown that the CPE is able to form pores in pure lipid bilayers in the absence of a receptor protein. Thus binding of CPE to host cell proteins to form complexes such as claudin is not a prerequisite for pore formation.

We noted the requirement for a relatively high concentration ($\sim 10$ μg) of CPE, and for relatively long periods of exposure. This contrasts with the rapid increases in short-circuit current recorded from Caco-2 cell monolayers in Ussing chambers at 37°C, which reached a maximum 3 min after the addition of $\sim 2$ μg CPE [10]. It is known that CPE (and other pore-forming toxins) aggregates when held at 4°C [14,15] and this may have contributed to the inefficiency of channel insertion. Membrane incorporation may also be relatively inefficient in the absence of specific 'receptors' such as claudins. Such proteins may act to localise the toxin at the bilayer/solution interface or assist insertion into the

membrane by promoting conformational changes in CPE (from β-sheet to an α-helical structure [16]). A mechanism of this type has been successfully tested for spider venom α-latrotoxin (α-LTX) and its cell-associated surface receptors, which appear to have no structural role in the pores formed by the toxin [17].

The first direct observation that CPE has ion channel activity was obtained by Sugimoto et al. using soybean asolectin bilayers [18]. In light of concern regarding the purity of soybean extracted asolectin, our results corroborate their findings. However, in contrast to the broad range of conductances (40–450 pS) reported by Sugimoto, we have found that the single channels described exhibit a narrow range of conductance values.

The well-defined channels we describe in this report exhibit many features that compare closely with our previous findings in Caco-2 cells [10]:

1. The currents in each case are carried predominantly by cations.
2. Voltage-dependent closure of the channels with increasing depolarisation ($> +30$ mV) mirrors the time-dependent closure of outward currents (in response to $> +40$ mV commands) observed in whole-cell patch-clamp recordings of Caco-2 cells.
3. The reduced permeability of single channels to organic cations (compared to $Na^+$) as the geometric diameters of the cations are increased corresponds to results obtained previously in Caco-2 monolayers in Ussing chambers.
4. The large cation *N*-methyl-D-glucamine is impermeant in single, whole-cell patch-clamp recordings and impermeant in single channels in bilayers.

Overall, our findings strongly suggest that CPE-induced changes in membrane permeability result from pores formed entirely by CPE without the requirement for activation of cell signalling pathways and distinct from any increases in paracellular conduction.

The role of mepacrine as a channel blocker is also potentially significant, because very few compounds are known to block toxin-induced pores in membranes. Mepacrine also blocks mammalian ion channels (end plate currents and the neuronal nicotinic

acetylcholine receptor [19,20]) in a similar manner, consistent with an 'open channel' mechanism of block. The effect of mepacrine on native tight junction function will be worth examining in future studies to discriminate between pore formation and paracellular changes.

In conclusion, we show that CPE-induced pores exhibit properties that correspond to ionic currents observed in intact monolayers and single cells in intestinal Caco-2 cells. In addition, host cell proteins such as claudin and occludin are not required structurally in the formation of CPE-induced pores. Instead, we speculate that such proteins may have a role in raising the local concentration of the toxin, and may even promote insertion of the toxin into the membranes of intestinal epithelia.

## Acknowledgements

## References

[1] B.A. McLane, Toxicon 34 (1996) 1335–1343.
[2] R. Skjelkvale, T. Uemura, J. Appl. Bacteriol. 43 (1977) 281–286.
[3] M. Matsuda, K. Ozutsumi, H. Iwahashi, N. Sugimoto, Biochem. Biophys. Res. Commun. 141 (1986) 704–710.
[4] E.U. Wieckowski, A.P. Wnek, B.A. McClane, J. Biol. Chem. 269 (1994) 10836–10848.
[5] J. Katahira, N. Inoue, Y. Horiguchi, M. Matsuda, N. Sugimoto, J. Cell Biol. 36 (1997) 1239–1247.
[6] K. Fujita, J. Katahira, Y. Horiguchi, N. Sonoda, M. Furuse, S. Tsukita, FEBS Lett. 476 (2000) 258–261.
[7] B.A. McClane, Trends Microbiol. 8 (2000) 145–146.
[8] U. Singh, C.M. Van Italle, L.L. Mitic, J.M. Anderson, B.A. McClane, J. Biol. Chem. 275 (2000) 18407–18417.
[9] N. Sonoda, M. Furuse, H. Sasaki, S. Yonemura, J. Katahira, Y. Horiguchi, S. Tsukita, J. Cell Biol. 147 (1999) 195–204.
[10] S.P. Hardy, M. Denmead, N. Parekh, P.E. Granum, J. Med. Microbiol. 48 (1999) 235–243.
[11] P.E. Granum, J.R. Whitaker, Appl. Environ. Microbiol. 39 (1980) 1120–1122.
[12] A.J. Williams, in: R.H. Ashley (Ed.), Ion Channels, a Practical Approach, IRL/OUP, Oxford, 1995, pp. 43–67.
[13] A. Schmid, R. Benz, I. Just, K. Aktories, J. Biol. Chem. 269 (1994) 16706–16711.
[14] G. Enders L, C.L. Duncan, Can. J. Microbiol. 22 (1976) 1410–1414.
[15] P.E. Granum, J.R. Whitaker, R. Skjelkvåle, Biochim. Biophys. Acta 668 (1981) 325–332.
[16] P.E. Granum, O. Harbitz, J. Food Biochem. 9 (1985) 137–146.
[17] K.V. Volynski, F.A. Meunier, V.G. Lelianova, E.E. Dudina, T.M. Volkova, M.A. Rahman, C. Manser, E.V. Grishin, J.O. Dolly, R.H. Ashley, Y.A. Ushkaryov, J. Biol. Chem. 275 (2001) 41175–41183.
[18] N. Sugimoto, M. Takagi, K. Ozutsumi, S. Harada, M. Matsuda, Biochem. Biophys. Res. Commun. 14 (1988) 551–556.
[19] R.P. Adams, A. Feltz, J. Physiol. 306 (1980) 261–281.
[20] S. Tamamizu, A.P. Todd, M.G. McNamee, Cell. Mol. Neurobiol. 15 (1995) 427–438.